Signature quality attributes of CD146+ mesenchymal stem/stromal cells correlate with high therapeutic and secretory potency

Annie C. Bowles, Dimitrios Kouroupis, Melissa A. Willman, Carlotta Perucca Orfei, Ashutosh Agarwal, Diego Correa

Received: 31 December 2019 | Accepted: 1 April 2020

DOI: 10.1002/stem.3196

Authored by a member of

IFATS International Federation for Adipose Therapeutics and Science

STEM CELLS

TRANSLATIONAL AND CLINICAL RESEARCH

Signature quality attributes of CD146$^+$ mesenchymal stem/stromal cells correlate with high therapeutic and secretory potency

Annie C. Bowles[1,2,3,4] | Dimitrios Kouroupis[1,2] | Melissa A. Willman[2] | Carlotta Perucca Orfei[5] | Ashutosh Agarwal[3,4] | Diego Correa[1,2,4]

[1]Department of Orthopaedics, UHealth Sports Medicine Institute, University of Miami, Miller School of Medicine, Miami, Florida

[2]Diabetes Research Institute & Cell Transplantation Center, University of Miami, Miller School of Medicine, Miami, Florida

[3]Department of Biomedical Engineering College of Engineering, University of Miami, Miami, Florida

[4]DJTMF Biomedical Nanotechnology Institute at the University of Miami, Miami, Florida

[5]IRCCS Istituto Ortopedico Galeazzi, Laboratorio di Biotecnologie Applicate all'Ortopedia, Milan, Italy

Correspondence
Diego Correa, MD, MSc, PhD, Department of Orthopaedics, UHealth Sports Medicine Institute, and Diabetes Research Institute & Cell Transplant Center, University of Miami, Miller School of Medicine, 1450 NW 10th Avenue (3014), Miami, FL.
Email: dxc821@med.miami.edu

Abstract

CD146$^+$ bone marrow-derived mesenchymal stem/stromal cells (BM-MSCs) play key roles in the perivascular niche, skeletogenesis, and hematopoietic support; however, comprehensive evaluation of therapeutic potency has yet to be determined. In this study, in vitro inflammatory priming to crude human BM-MSCs (n = 8) captured a baseline of signature responses, including enriched CD146$^+$ with coexpression of CD107a^{High}, CXCR4^{High}, and LepR^{High}, transcriptional profile, enhanced secretory capacity, and robust immunomodulatory secretome and function, including immunopotency assays (IPAs) with stimulated immune cells. These signatures were significantly more pronounced in CD146$^+$ (POS)-sorted subpopulation than in the CD146$^-$ (NEG). Mechanistically, POS BM-MSCs showed a markedly higher secretory capacity with significantly greater immunomodulatory and anti-inflammatory protein production upon inflammatory priming compared with the NEG BM-MSCs. Moreover, IPAs with stimulated peripheral blood mononuclear cells and T lymphocytes demonstrated robust immunosuppression mediated by POS BM-MSC while inducing significant frequencies of regulatory T cells. in vivo evidence showed that POS BM-MSC treatment promoted pronounced M1-to-M2 macrophage polarization, ameliorating inflammation/fibrosis of knee synovium and fat pad, unlike treatment with NEG BM-MSCs. These data correlate the expression of CD146 with innately higher immunomodulatory and secretory capacity, and thus therapeutic potency. This high-content, reproducible evidence suggests that the CD146$^+$ (POS) MSC subpopulation are the mediators of the beneficial effects achieved using crude BM-MSCs, leading to translational implications for improving cell therapy and manufacturing.

KEYWORDS

CD107a, CD146, immunomodulation, infrapatellar fat pad fibrosis, macrophage polarization, mesenchymal stem/stromal cells, synovitis

1 | INTRODUCTION

The unique qualities inherent to mesenchymal stem/stromal cells (MSCs) still warrant detailed investigation into the dynamic responses induced by various molecular cues that influence their functional capacity, or therapeutic potency. Initially, in vitro multilineage differentiation capacity of MSCs guided researchers to cell engraftment and replacement strategies; however, we now recognize the innate

paracrine signaling and immunomodulatory capacity of these cells as mechanisms to facilitate local changes in various milieus.[1-3] The constitutively active functions of MSCs are modulated by the surrounding environment, which informs MSCs of spatial and temporal cues.[4,5] In response, MSCs produce a tailored profile of secreted factors, including proteins, microRNAs, and extracellular vesicles instructive and conducive to the milieu, leading to the understanding that the efficacy of MSCs lies mainly in the comprehensive potency of its secretome.[6,7]

The responsiveness of MSCs has led to directing responses in vitro through cell priming or preconditioning.[8] Subsequent interrogations of the cells and associated secretomes help correlate those responses with in vivo outcomes and explore ways to enhance MSC potency.[9-11] These dynamic features, including the immune cell-like responsiveness, secretory capacity, high migratory potential, and immunomodulatory cross talk, along with their unique stem-like state and clonal reproducibility have made it difficult to distinguish MSCs beyond the minimum International Society of Cell and Gene Therapy (ISCT) criteria.[12,13] Consequently, the once regarded "unique cell" dogma has changed, redefining "mesenchymal stem cells" to "multipotent mesenchymal stromal cells" as stated by ISCT in 2005[14] and later described as "medicinal signaling cells."[15]

The perivascular prevalence of MSC in most tissues has led to the proposal of MSC and pericytes as developmentally related.[5,16] Compelling evidence has demonstrated that MSCs and pericytes do, in fact, share similar phenotypic markers (eg, CD146, NG2, PDGF-Rβ), the perivascular niche, differentiation potential, and functional effects regarding tissue homeostasis and immunomodulation.[17-21] Within the bone marrow (BM), CD146 expression developmentally discriminates the bone and stroma from similar progenitors arising from skeletal stem cells,[22] as well as perivascular from bone-lining/endosteal bone marrow-derived mesenchymal stem/stromal cells (BM-MSCs), all exhibiting osteogenic and hematopoietic support capabilities.[23-25] $CD146^+$ BM-derived perivascular MSC are further discriminated based on nestin and leptin receptor (LepR) expression,[26-28] capable of forming heterotopic ossicles.[29] Finally, $CD146^+$ pericytes, along with $CD34^+$ adventitial cells within the perivascular space[30] have been collectively called perivascular stem/stromal cells (PSC), suitable for bone reconstruction.[31-33]

By investigating CD146 expression on MSC, our objective is to not only shed light on the ambiguity of MSC phenotypes but also provide compelling evidence of additional, less-known signatures relative to the unique immunomodulatory subpopulation of MSC with functions beyond the aforementioned roles. We then hypothesize that a specific subset of MSC located within the perivascular niche ($CD146^+$) would exhibit more robust responses to insults and inflammatory cascades than MSC otherwise more distant from vascular structures ($CD146^{-/low}$). Additional correlative signature markers we describe with $CD146^+$ BM-MSCs are CD107a, CXCR4, and LepR. CD107a, or lysosomal-associated membrane protein-1(LAMP-1), is a marker of highly secretory cytotoxic T cells and actively degranulating natural killer cells,[34-39] but largely unknown in MSCs, yet may correlate with secretory capacity (eg, paracrine activity). CXCR4 and its cognate ligand SDF-1/CXCL12 form a well-documented axis mediating migration of MSC in response to sites of injury.[8,40] Leptin has been associated with energy regulation[41] and bone remodeling,[42] signaling through LepR in the hypothalamus and BM cells, and modulation of osteogenic and adipogenic differentiation of MSCs in the bone.[43]

By selection, we propose to reduce heterogeneity of isolated MSCs, while characterizing a more uniform, robust, and highly responsive cell subpopulation implicated behind the beneficial effects of a crude (ie, unfractionated [UNF]) MSC preparation. Herein, we showed that human BM-MSC (n = 8) crude population, or UNF BM-MSC, exhibited novel phenotypic (eg, $CD107a^+$) and transcriptional signatures (eg, leukemia inhibitory factor [*LIF*]) after inflammatory priming, which correlated with the high-content analysis of a higher secretory profile and reduced variability in the $CD146^+$ (POS)-sorted subpopulation compared with the $CD146^-$ (NEG) subpopulation. Upon inflammatory priming, numerous protein mediators were released at markedly higher levels by the POS subpopulation, suggesting a significantly more rapid and robust immunomodulatory response, correlative with reduced proliferation of stimulated target immune cells in vitro. These responses were further translated using a rat model of acute inflammation/fibrosis of the joint synovial membrane and fat pad, where an intra-articular injection of POS cells consistently resulted in greater therapeutic efficacy compared with the marginal effects with the NEG fraction by promoting M2 macrophages polarization in vivo. Mechanistically, the therapeutic difference related to more M2-like (ie, alternative activation) macrophages was indicative of anti-inflammation and repair mechanisms at the synovium and fat pad.

Together, this deep investigational approach into evaluating the MSC programs attributed to the pericyte marker CD146 provides compelling evidence that the $CD146^+$ BM-MSC subpopulation constitutes the innately therapeutically cells with high secretory capacity. Further, this evidence suggests $CD146^+$ BM-MSC subpopulation as the facilitators among the crude MSC population, underrepresented by the nonselective isolation process. Immediate implications relate

Significance statement

Cell therapies for comprehensively treating numerous clinical indications are on the rise. With the advances to manufacturing and commercialization, signature quality attributes relative to functional potency are necessary indicators of therapeutic efficacy for cell selection optimization. This study demonstrates compelling evidence for a subpopulation of mesenchymal stromal/stem cells (MSCs) that are suggested to be the mediators of the beneficial effects achieved by crude MSCs. These results translate into techniques useful for determining cell qualities and functional capacities, optimizing therapeutic cell selection for efficient manufacturing, and mechanisms of action mediated by cell therapy for the treatment of joint inflammation and fibrosis.

with uniformity during cell-based product manufacturing, more reproducible outcomes, and improving precision for defining mechanistic underpinnings for bench-to-bedside translation.

2 | RESULTS

2.1 | MSC characterization of human donors BM-MSC

BM-MSCs from eight donors of both sexes (36.5 ± 9.8 years of age) (Figure S1A) were evaluated by standard characterization assays to validate MSC qualities (Figure S1). Quantitative analysis of BM-MSC expressions included frequencies of positive surface markers CD105 (99.55% ± 0.25%), CD90 (97.64% ± 1.21%), CD73 (98.95% ± 1.02%), and CD44 (98.26% ± 1.42%) and negative surface markers CD34 (0.43% ± 0.37%), CD31 (0.53% ± 0.30%), CD45 (0.53% ± 0.30%), CD31 (0.3% ± 0.20%), and HLA-DR (0.58% ± 0.36%; Figure S1C). Quantification of Oil Red O, alizarin red, and glycosaminoglycans/Alcian blue demonstrated BM-MSC multipotency for induced adipogenesis (2.00 ± 0.32 normalized optical density [OD]), osteogenesis (3.83 ± 1.40 normalized OD), and chondrogenesis (26.53 ± 10.85; Figure S1D). Morphological and growth kinetics were indicative of BM-MSCs (Figure S1B,E). Growth kinetics showed slight alterations in donors 1, 4, and 6 depicting a response upon priming resulting in an initial delayed proliferation to reveal donor-specific differences (Figure S1E).

2.2 | Signature profiles define human BM-MSC responses to inflammatory priming

Priming with inflammatory mediators mounted several measurable responses by BM-MSC. By profiling markers beyond those used as standard characterization to define MSC, all BM-MSC groups were interrogated for signatures of surface markers, which could indicate an alternate state and/or activity, given the increased expression of the selected markers upon inflammatory priming. The expression of marker CD146 was increased from 50.14% ± 15.50% on UNF Naïve to 60.10% ± 18.44% ($P < .05$) on UNF Primed BM-MSC (Figure 1A). Surface CD107a expression markedly increased from 9.70% ± 6.07% on UNF Naïve to 43.68% ± 21.43% ($P < .01$) on UNF Primed BM-MSC, while CXCR4 increased from 11.50% ± 9.72% on UNF Naïve to 38.47% ± 17.55% ($P < .01$) on UNF Primed BM-MSC. LepR expression increased from 5.09% ± 1.97% to 28.55% ± 15.28% ($P < .01$) on UNF Naïve to UNF Primed BM-MSC, respectively (Figure 1B). Coexpression of primary signature marker CD146 with CD107a, CXCR4, or LepR led to an increased expression of 9.73% ± 8.06% to

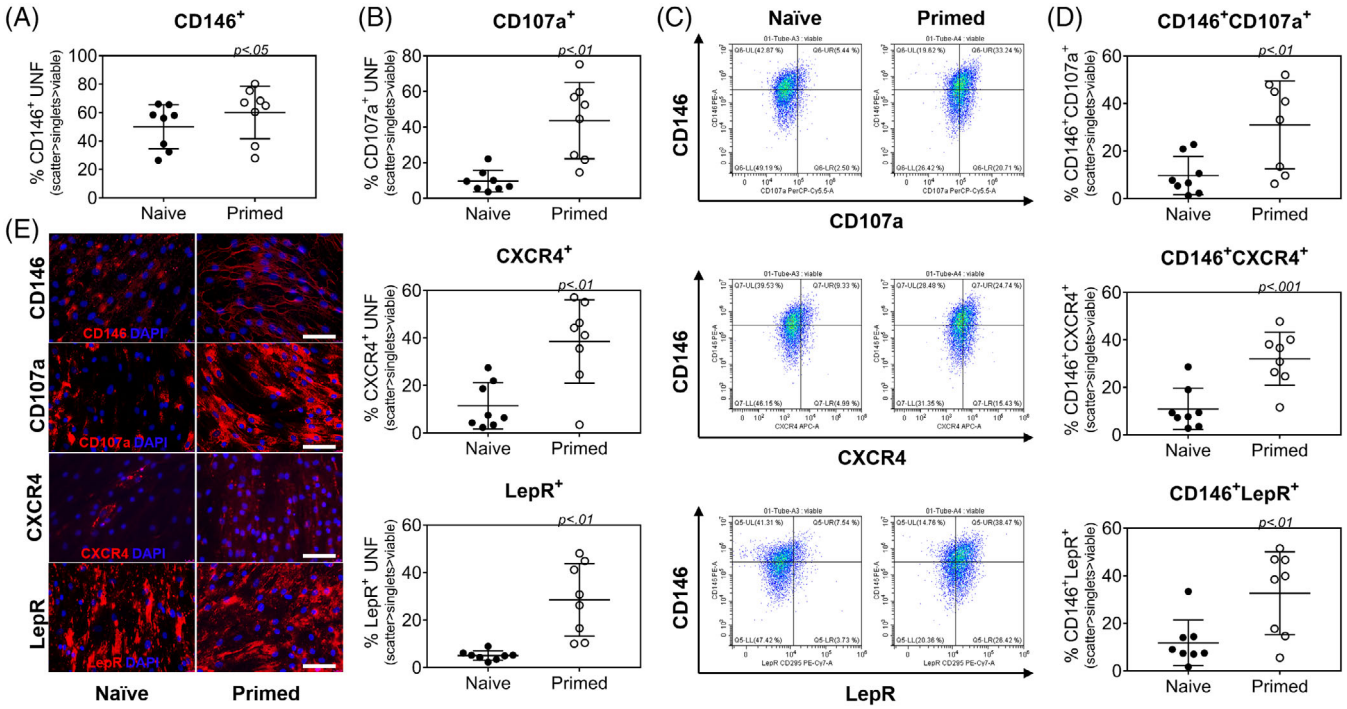

FIGURE 1 Unfractionated (UNF) BM-MSC expressed enrichment of defined signature markers upon priming with inflammatory mediators. A, CD146 was designated as a highly distinguishable marker for a potently immunomodulatory BM-MSC subpopulation as extracellular expression was markedly increased in all UNF BM-MSC donors (n = 8) when primed. B, Additional markers of interest used to distinguish a signature profile of immunomodulatory BM-MSC which expressions are consistently enhanced by priming. C,D, Images and quantitative analysis of the coexpressions of CD146 and designated immunomodulatory markers supported the signature markers highly enriched on a specific subpopulation of BM-MSCs. E, Immunofluorescence of signature markers show constitutive expressions on UNF Naïve and increased expression in the UNF Primed. Scale bars = 50 μm. Values are presented as mean ± SD. BM-MSC, bone marrow-derived mesenchymal stem/stromal cell

31.08% ± 18.52% ($P < .01$) for $CD146^+CD107a^+$, 10.97% ± 8.69% to 32.05% ± 11.17% ($P < .001$) for $CD146^+CXCR4^+$, and 11.83% ± 9.62% to 32.67% ± 17.40% ($P < .01$) for $CD146^+LepR^+$ on UNF Naïve to UNF Primed BM-MSC, respectively, suggesting a reproducible signature phenotype upon inflammatory priming in all donors (Figure 1C, D). Fluorescence images show the increased antigen presentation of each signature marker on UNF Naïve and Primed cohorts (Figure 1E; antibody controls in Figure S6A).

2.3 | Priming induced immunomodulatory BM-MSC functions defined by secretory and transcription profiles

Immunomodulatory function was elicited by a response by inflammatory priming of BM-MSCs, which was deduced by profiling secreted proteins and transcriptional changes. Numerous proteins were quantitatively compared between UNF Naïve and Primed cohorts (Figure S2A). Corroboration of the significantly altered proteins of the UNF Primed profile with pathway analysis further supported robust immunomodulatory signaling with the top three relevant pathways matched as interleukin-10 (IL-10; *HSA-6783783*), toll-like receptor (hsa04620), and IL-4 and IL-13 (HSA-6785807) signaling pathways (Figure S2B). Immunomodulatory activities facilitated by prostaglandin E-2 (PGE-2) and indoleamine 2,3-dioxygenase (IDO) were suggested to strongly influence the functional effects of the UNF Primed BM-MSC which were measured significantly higher (3.73 ± 3.03-fold and 5.12 ± 3.39-fold) compared with UNF Naïve cohorts, respectively (Figure S2C).

Similarly, the transcription profiles of genes revealed a consistent shift in overexpressed and underexpressed gene transcripts in the UNF Primed BM-MSCs compared with the UNF Naïve cohort induced by the inflammatory priming (Figures S2D and S5A). Of these, UNF Primed BM-MSC showed upregulation of *LIF* (3.92-fold; $P < .0013$), indicative of a highly immunosuppressive/tolerogenic immunity state and stemness.[44,45] Contrastingly, the three master regulators of mesenchymal differentiation programs were significantly downregulated, namely *RUNX2* for osteogenesis (−4.11-fold; $P < .0012$), *SOX9* for chondrogenesis (−2.91-fold; $P < .012$), and *PPARγ* for adipogenesis (−2.49-fold; $P < .048$; Figure S2D). Interestingly, various other transcripts associated with those programs (eg, *COL1A1*, *GFD5*, *BMP6*, *BGLAP*, *TGFβ1-3*, *ITGB1*) were similarly downregulated (Figures S2D and S5A).

2.4 | Immunomodulatory potency of UNF Primed BM-MSC mitigated immune cell proliferation and differentiation

Several molecules such as IL-10,[46] PGE-2,[47] and IDO[9,11] have been examined to suggest potency of MSC, but given the robust secretory repertoire of MSC, a single molecular assessment is inadequate. In this study and several others,[46,48] potency corresponded to diminished proliferation of stimulated immune cells, peripheral blood mononuclear cells (PBMC) and T lymphocytes (T cell), when cocultured with BM-MSC.[48,49] We further analyzed specific subsets of T cells to determine whether immunomodulatory potency yielded more compelling implications.

According to the immunopotency assay (IPA) matrix (Figure S3), a dose-response evaluation of PBMC stimulated with phorbol myristate acetate (PMA)/ionomycin cocktail for a robust proliferative response was performed to distinguish the ratios and suppressive effects of UNF Naïve and UNF Primed BM-MSC. This evidence indicated that a 2:1 PBMC to BM-MSC ratio was optimal for achieving a significantly attenuated proliferative response of stimulated PBMC (no BM-MSC; 37.50% ± 9.98%) by coculture with UNF Naïve (21.00% ± 19.61%; $P < .01$) and, more so, UNF Primed BM-MSC (12.25% ± 11.62%; $P < .001$). Higher ratios of PBMC to UNF Naïve BM-MSC progressively reduced the effects, measured at 4:1 (43.25% ± 21.00%), 12:1 (76.75% ± 10.75%), and 60:1 (78.00% ± 10.92%). UNF Primed cohorts, on the other hand, produced a stronger immunosuppressive response at 4:1 (4.75% ± 1.71%; $P < .0001$), 12:1 (22.75% ± 30.30%; $P < .05$), and 60:1 (72.50% ± 8.10%) ratios, overcoming the dose-dependent reducing effect observed with UNF Naïve BM-MSC (Figure S4A).

To complement, pan T cells were cocultured (2:1) with the same BM-MSC groups. T cells were stimulated with a CD3/CD28 antibody cocktail, which mimics a physiological activation by antigen-presenting cells[50] that warrants a minimal proliferative response over the 3-day IPA according to the experimental design (Figure S3). Control T cells (no BM-MSC) had a proliferation rate of 11.56% ± 8.86%, significantly increased with coculture with UNF Naïve BM-MSC (32.11% ± 16.85%, $P < .05$) but not with UNF Primed cohorts (20.30% ± 17.62%; Figure S4B,C), suggesting an immunosuppressive effect of the latter. Given the coculture cell ratios used, the presence of BM-MSCs was expected to increase T-cell proliferation.[51] However, a more detailed description of the proliferating cells was visualized as scatter patterns gated as parent T cells (carboxyfluorescein succinimidyl ester, $CFSE^{high}$) and progeny T cells ($CFSE^{low}$) using flow cytometric analysis for quantification of proliferation rates and phenotypic subsets (Figure S4C,D). Interestingly, despite the increased number of total proliferating T cells described (Figure S4B), the number of progenies visualized was reduced with UNF Naïve and more so with UNF Primed BM-MSC, suggesting reduced numbers of actual cell divisions during the coculture (Figure S4C).

Stimulated T cells cocultured with UNF Naïve (13.18% ± 3.83%; $P < .001$) and UNF Primed (12.82% ± 1.65%; $P < .01$) BM-MSCs were significantly higher in frequency of $CD3^+CD4^-CD8^-$ T cells than controls (7.16% ± 3.14%), suggesting modulated differentiation by both UNF BM-MSC cohorts rendering T cells of alternate subsets that were not further defined (Figure S4D). The decreased trend of cytotoxic T cells resulting from the IPA with UNF Naïve (27.24% ± 9.70%) and UNF Primed (26.50% ± 3.73%) BM-MSCs compared with no-BM-MSC controls (30.35% ± 17.03%) suggested that BM-MSCs did not bolster differentiation of $CD3^+CD8^+$ cytotoxic T cells. IPA results showed that UNF Primed BM-MSCs substantially reduced the differentiation to $CD3^+CD4^+$ helper T cells to 45.50% ± 9.00% ($P < .05$) compared with

controls (60.78% ± 12.88%), while UNF Naïve cohorts (48.65% ± 7.66%) slightly mitigated helper T cell differentiation. Moreover, the percent of regulatory T-cell (Treg) subsets ($CD3^+CD4^+CD25^+foxp3^+$) induced within the helper T-cell population were markedly enhanced by the coculture with UNF Naïve (28.48% ± 19.45%; $P < .05$) and UNF Primed (25.36% ± 22.63%) BM-MSC compared with no BM-MSC controls (5.56% ± 3.87%; Figure S4D). Time-lapse analysis further demonstrated the proliferation responses of each T-cell group during the IPA by CFSE detection (Figure S4E).

2.5 | POS BM-MSC express an enrichment of signature markers

To substantiate the immunomodulatory potency of BM-MSC related directly to expression of CD146, magnet-activated cells sorting (MACS) was used to fractionate UNF BM-MSC (n = 3) into CD146+ (POS) and CD146– (NEG) fractions, which were subsequently interrogated by similar approaches performed on UNF BM-MSC. CD146-based MACS yielded POS (71.01% ± 7.03%) and NEG (18.82% ± 5.69%; $P < .05$) subpopulations with marked differences in CD146 expression, although suboptimal for capturing pure subpopulations (Figure 2A).

Phenotypic analysis corresponding to Naïve and Primed cohorts of POS and NEG BM-MSC subpopulations supported the enrichment of signature markers when exposed to inflammatory priming similar to the UNF cohorts. CD146 expression was detected in the POS Naïve (84.45% ± 6.11%) and NEG Naïve (16.08% ± 6.12%) cohorts, which was further enriched with priming in both the POS Primed (91.9% ± 6.49%; $P < .05$) and NEG Primed (23.44% ± 8.93%) cohorts. Highly significant differences remained between the POS Naïve and NEG Naïve ($P < .0001$) and the POS Primed and NEG Primed ($P < .0001$) cohorts (Figure 2B).

Expression of CD107a was significantly increased in both the POS (36.51% ± 17.76%; $P < .05$) and NEG (21.77% ± 13.21%; $P < .05$) with priming, compared with the corresponding POS (15.09% ± 9.64%) and NEG (8.87% ± 6.03%) Naïve cohort, respectively, showing a higher expression in the POS group overall. Similarly, CXCR4 and LepR expressions were increased with priming in both the POS and NEG BM-MSC subpopulations. POS Naïve BM-MSC (15.31% ± 12.24%) expression of CXCR4 increased to 35.70% ± 20.38% on POS Primed cohorts, while NEG Naïve (8.85% ± 7.28%) was increased to 24.11% ± 16.85% on NEG Primed cohorts. Modest enrichment of LepR was measure from 13.16% ± 15.97% expression on the POS Naïve to 30.18% ± 27.29% on POS Primed and remained comparable between NEG Naïve (6.33% ± 8.04%) and NEG Primed (12.19%

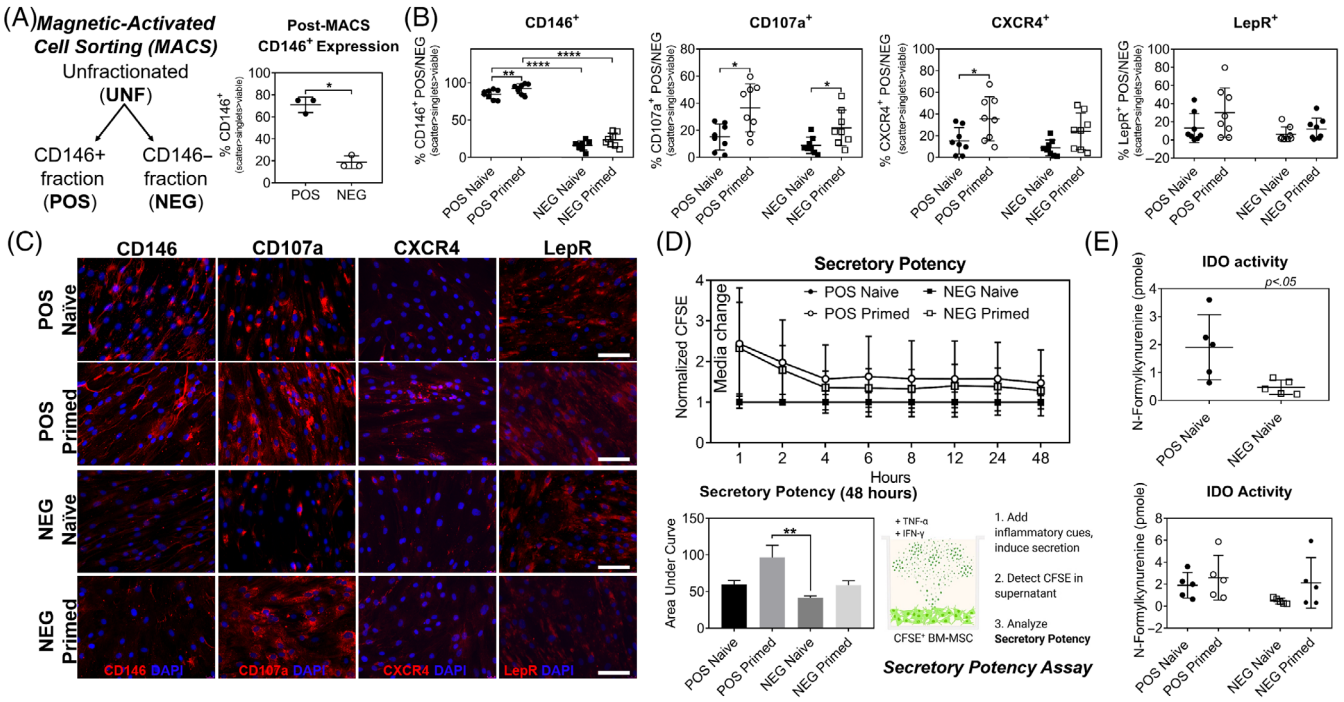

FIGURE 2 Sorting by CD146 revealed inherent features associated with $CD146^+$ (POS) and $CD146^-$ (NEG) BM-MSC. A, Magnet-activated cell sorting (MACS) was used to capture $CD146^+$ (POS) and $CD146^-$ (NEG) BM-MSC. B, Signature marker were differentially expressed and enriched in Naïve and Primed cohorts of POS and NEG BM-MSC (n = 8). C, Immunofluorescence of signature markers on the extracellular membranes of POS and NEG BM-MSC. D, Secretory potency was measured as total secreted molecules and represented as time-lapse secretion as well as the area under curve for the 48-hour duration of priming (n = 4). E, IDO activity compared between the Naïve cohorts of POS and NEG BM-MSCs (above) and Naïve and Primed cohorts of POS and NEG BM-MSCs (below). Scale bars = 50 μm. Values are presented as mean ± SD. *$P < .05$; **$P < .01$; ***$P < .001$; ****$P < .0001$. BM-MSC, bone marrow-derived mesenchymal stem/stromal cells; IDO, indoleamine 2,3-dioxygenase stem/stromal cells

± 11.88%) BM-MSC (Figure 2B). Fluorescence images of POS and NEG BM-MSC validated the increased expression of signature markers as Naïve BM-MSC compared with Primed cohorts at 48 hours of inflammatory priming (Figure 2C).

2.6 | Secretory potency and profile of POS BM-MSCs was most robust and immunomodulatory

Overall secretory activity was measurable by using CFSE labeling of BM-MSCs, which in turn, covalently linked to intracellular residues.[52] By fluorescence detection of the conditioned media, CFSE-labeled contents secreted by the BM-MSCs were captured, and the mounted secretory response upon inflammatory priming observed in the Primed cohorts were quantified and normalized to the corresponding Naïve cohorts over time. The change of media at hour 0 containing the inflammatory stimuli resulted in a large bolus of CFSE-labeled contents released by both POS Primed and NEG Primed BM-MSCs that was measured at hour 1 which gradually tapered off by hour 4. Consistently, Primed BM-MSCs released a higher total of contents throughout the detected time points of the 48-hour priming period. Secretory release by hour 4 had equilibrated the cells to constitutive release measured by POS Primed (1.57-fold) and NEG Primed (1.36-fold) and remained steady until a final drop to comparable levels of the Naïve cohorts at 48 hours (Figure 2D, top). To further validate the larger potency of the POS subpopulation compared with the NEG subpopulation, the cumulative secretory potency of each BM-MSC group was quantitatively compared. POS Naïve (59.38 ± 11.65) and POS Primed (96.58 ± 32.88; $P < .05$) groups generated a more robust secretory release over 48 hours than released by NEG Naïve (41.38 ± 5.35) and NEG Primed (58.83 ± 11.97) groups (Figure 2D, bottom). In fact, the constitutive secretory release of contents of the POS Naïve group was comparable to the amount released by the NEG Primed cohort over the 48 hours underlining the greater secretory potency of the POS subpopulation over the NEG subpopulation. Interestingly, this secretory profile mirrors the expression profile of CD107a in all groups, supporting the correlation between phenotype and function.

To elucidate the molecules that contribute to the compelling secretory data distinguishable of the POS subpopulation, analyses of immunomodulatory PGE-2, and IDO activity were measured to substantiate potency. Constitutive IDO activity, indirectly measured by metabolized tryptophan (Trp), NEG Naïve BM-MSC was measured as 0.47 ± 0.26 pmol ($P < .05$) which was significantly less than the activity measured by POS Naïve (1.90 ± 1.16 pmol). As reported by UNF BM-MSC, inflammatory priming further enhanced IDO activity with POS Primed increasing to 2.59 ± 2.03 pmol and NEG Primed to 2.12 ± 2.3 pmol (Figure 2E).

Heat map representation of the relative fold changes between the Primed and Naïve cohorts of the UNF, POS, and NEG BM-MSC demonstrated the largest increases among the inflammation-related growth factors and cytokines corresponding to the POS Primed group (Figure 3A,B). Moreover, quantitative comparisons were presented individually of pertinent immunomodulatory proteins secreted by each Primed cohort normalized to the Naïve cohort of the UNF, POS, or NEG BM-MSC. Of the most significant proteins, the POS Primed secreted the highest levels of transforming growth factor-β1 (TGF-β1; 3.22-fold; $P < .0001$), soluble tumor necrosis factor receptor 2 (sTNF-R2; 2.61-fold; $P < .01$), macrophage inflammatory protein-1α (MIP-1α; 4.33-fold; $P < .01$), platelet derived growth factor-BB (PDGF-BB; 1.46-fold; $P < .05$), IL-10 (1.84-fold; $P < .05$), interleukin-12 p40 (IL-12 p40; 1.57-fold; $P < .05$), interleukin-13 (IL-13; 1.88-fold; $P < .05$), interleukin-15 (IL-15; 1.73-fold; $P < .05$), and macrophage-colony stimulating factor (M-CSF; 1.31-fold; $P < .05$). Macrophage chemotactic protein-2 (MCP-2) and regulated upon activation, normal T-cell expressed, and secreted were both significantly greater in the supernatants of the UNF Primed measured as 84.71-fold ($P < .0001$) and 28.75-fold ($P < .05$) and POS Primed measured as 54.05-fold ($P < .001$) and 19.49-fold ($P < .05$), respectively. Priming induced the largest secretory increases of intracellular adhesion molecule-1 (ICAM-1), interleukin-8 (IL-8), and interferon-γ (IFN-γ) in all BM-MSC groups, which are suggested to be direct targets of the exogenous IFN-γ and TNF-α used in the priming cocktail. ICAM-1 was highest in the supernatant of POS Primed groups (9.20-fold; $P < .001$) followed by NEG Primed (8.14-fold; $P < .01$) and UNF Primed (6.92-fold; $P < .05$) while IL-8 was highest in the UNF Primed groups (9.74-fold; $P < .001$) followed by NEG Primed (8.16-fold; $P < .01$) and POS Primed (7.54-fold; $P < .05$). Although detection of IFN-γ included secreted and exogenous protein from the priming cocktail, the levels were comparable in the UNF Primed (11.31-fold; $P < .001$), POS Primed (10.19-fold; $P < .001$), and NEG Primed (9.56-fold; $P < .001$) BM-MSCs (Figure 3C).

Of the 16 proteins discussed that were measured as significantly greater from at least one of the Primed cohorts of UNF, POS, or NEG BM-MSC, 14 were from the POS BM-MSC subpopulation, supporting its robust and comprehensive secretory profile in response to inflammatory priming. Pathway associations with all significantly altered proteins reveal differences in the signaling pathways between subpopulations, where rheumatoid arthritis (RA)-associated (hsa05323), Jak-STAT (hsa04630), TNF (hsa04668), and interleukin-17 (hsa04657) pathways were the top matches as modulated by the POS subpopulation, and not the NEG (Figure 4A, top). All three groups shared only four altered factors. Furthermore, unlike with UNF (2) and NEG (2), several of the altered factors (10) were exclusively altered in the POS group. POS shared more with the UNF (6) than with NEG (3), while NEG did not coincide with UNF in any response. This suggests a selective contribution of the POS within crude preparations to the immunomodulatory signaling for mechanistic targets and insight, especially related to inflammation and autoimmunity. Radar profile graphs from categorized signaling activities show high similarities and alignment between the UNF and POS subpopulation in both biological process and Reactome, especially with effects on leukocyte proliferation (GO:0070663) and TNF signaling (hsa04668) (Figure 4A, middle and bottom).

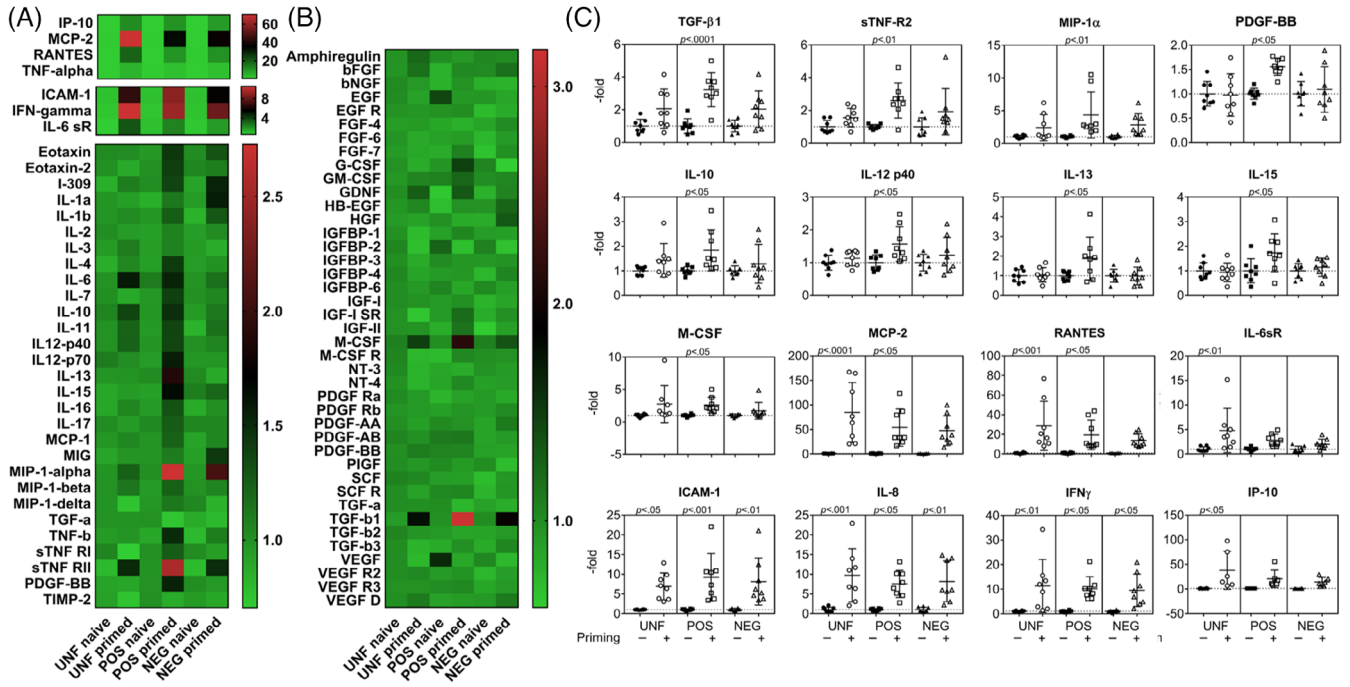

FIGURE 3 Secretory profiles support that the POS BM-MSC are the potent responders to inflammation. A,B, Fold change differences between the Naïve and Primed cohorts of the UNF, POS, and NEG groups (n = 8) reveal profiles indicating the largest secretory profiles of inflammatory and growth factor mediators by the POS BM-MSC with priming. C, Protein mediators determined to have the most significant differences among each group, highlighting the most robust changes of immunomodulatory factors by the POS BM-MSC. BM-MSC, bone marrow-derived mesenchymal stem/stromal cells; UNF, unfractionated

2.7 | Transcription profiles reveal signatures distinguishable of both subpopulations

Comprehensive strategies to determine the influence of the POS or NEG subpopulations within the cumulative UNF BM-MSCs are necessary to understand the contribution of each that may guide investigations to reducing heterogeneity for more consistent outcomes. The transcription profiles compared the genes actively overexpressed or underexpressed following priming in each BM-MSC group (Figure 4B; all values reported in Figure S5B). Among the UNF, POS, and NEG groups, all Primed cohorts consistently shared six overexpressed (>2-fold, $P < .05$) and six underexpressed (<−2-fold, $P < .05$) genes following priming, building a basis of expected overall transcriptional results for the crude population. In descending order, these included increased gene expressions of *ICAM-1*, *IL-1β*, *IL-6*, *BMP-2*, *TNF-α*, and *LIF*, and in ascending order of downregulated genes were *GDF5*, *COL1A1*, *BMP6*, *ITGAV*, *TGF-β3*, and *THY1*. These 12 genes were similarly altered, suggesting that although these subpopulations were distinguishable in phenotype and function, both POS and NEG subpopulations fundamentally show similarities in most gene expressions in response to priming (Figure 4B,C). However, critical transcriptional differences were indeed identified that correlate with functions ascribed specifically to $CD146^+$ BM-MSC. For instance, the master regulators and various other genes closely related to osteogenic and adipogenic differentiation potential (ie, *Runx2*, *PPARγ*, *BGLAP*, and *ITGB1*), initially found downregulated in UNF Primed cells (Figure S2D), were found altered only in the NEG Primed group. This suggests that POS Primed cells, despite the priming, retain their molecular osteogenic and adipogenic machinery[29,53] and that the suppression observed in the heterogeneous UNF Primed preparation can be attributed only to the NEG subpopulation. Furthermore, the POS Primed subpopulation showed additional signature gene expressions that revealed genes that may have larger implications. *BDNF* (3.58-fold; $P < .005$) was overexpressed and *GDF15* (−4.06-fold; $P < .03$) and *NUDT6* (−2.41-fold; $P < .01$) were underexpressed in only the POS Primed subpopulation whereas no unique genes were related to the NEG subpopulations. Primed cohorts of the UNF and POS BM-MSC shared significantly upregulated gene *VCAM1* and downregulated genes *PDGF-Rβ* and *TGF-β1* following inflammatory priming (Figure 4C).

2.8 | Potency and immunomodulatory function of POS subpopulation support the signature profile

Potency associated with the POS or NEG subpopulations, as with the UNF BM-MSCs, was determined by the most robust suppression of proliferation of stimulated target cells using the IPA. Dosage responses using PBMC showed the most significant reduction in proliferation rates at 2:1 ratio of PBMC cocultured with the POS Naïve (17.00% ± 13.59%; $P < .001$), POS Primed (7.75% ± 8.54%; $P < .0001$), NEG Naïve (16.25% ± 14.61%; $P < .001$), and NEG Primed

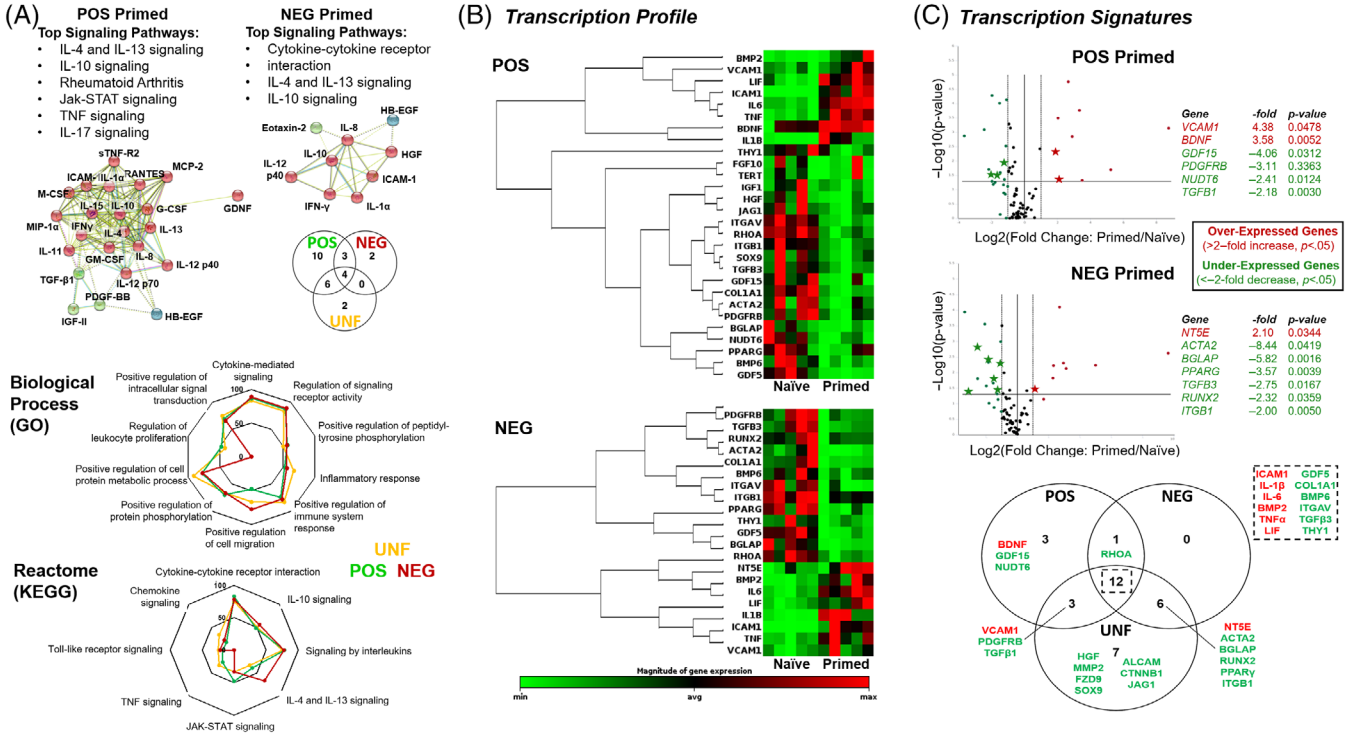

FIGURE 4 Pathway analysis of secreted proteins and transcriptional profiles. A, Highly regulated proteins (>1.4-fold increase and <−1.4-fold decrease) were oriented with STRING to derive the involvement of relevant pathways. Venn diagram, biological process, and Reactome associates exhibit the distinctive properties and the shared overlaps among the UNF, POS, and NEG BM-MSC. B, Unsupervised hierarchical cluster diagrams representing transcriptional profiles of the POS and NEG subpopulations in response to inflammatory priming show distinguishable difference leading to identification of key transcripts that are key associations with the specific subpopulation. C, Volcano plots derive transcriptional signatures differentially and specifically expressed by POS and NEG BM-MSC upon priming. Venn diagram further displays the strong functional influence of the POS subpopulation underlying the UNF BM-MSC. Stars represent statistical significance with values greater than 2-fold or less than −2-fold change. BM-MSC, bone marrow-derived mesenchymal stem/stromal cells; UNF, unfractionated

(9.88% ± 9.92%; $P < .001$). More importantly, at 4:1 POS Naïve (39.00% ± 17.38%; $P < .05$) and POS Primed (5.50% ± 5.20%; $P < .0001$) significantly outperformed the immunosuppressive potential of NEG Naïve (36.13% ± 30.93%) and NEG Primed (13.38% ± 14.26%; $P < .001$) subpopulations. Moreover, PBMC proliferation was significantly suppressed at 12:1 by the POS Primed (17.50% ± 8.81%; $P < .001$) and to lesser extent NEG Primed (22.63% ± 20.37%; $P < .01$) cohorts (Figure 5A).

Comparisons of the T-cell IPA results from the Naïve cohorts of the UNF, POS, and NEG BM-groups demonstrated the intrinsic contributions of the subpopulations within the UNF BM-MSC, explaining the results presented in Figure S4B. The increased T-cell proliferation observed with the UNF Naïve cohort (32.11% ± 16.85%) can now be exclusively attributed to the NEG fraction. Unlike the T-cell proliferation rate reduction to 16.72% ± 18.75% with the POS Naïve cohort (comparable to the no BM-MSC controls with T cells only 11.56% ± 8.86%; Figure 5C), a significantly higher rate was observed with the NEG Naïve cohort reaching 42.62% ± 7.87% ($P < .01$) (Figure 5B). Although donor-specific variations are observable, especially within the POS Naïve cohort, the reproducibility of this assay still showed a remarkable pattern among cohorts using the same donors in all groups. To further demonstrate the intrinsic immunosuppressive potency of the POS subpopulations, the POS Primed (12.81% ± 15.91%) showed no difference to the POS Naïve cohort in T-cell proliferation rates (Figure 5B,C), suggesting that the POS subpopulation is innately equipped to functionally immunomodulate, regardless of priming. The NEG Primed cohort was also able to reduce T-cell proliferation (13.24% ± 8.55%). However, when compared with the NEG Naïve rates, the necessity of a prior inflammatory priming for this subset to functionally perform becomes evident.

As demonstrated with the UNF groups (Naïve and Primed), a detailed description of the subsets of differentiated T cells is necessary to obtain a more complete picture of the immunomodulatory effect of the POS and NEG subpopulations. POS Naïve (15.76% ± 6.75%; $P < .05$) and POS Primed (16.75% ± 6.95%; $P < .01$) BM-MSC groups coincided with markedly higher frequencies of $CD3^+CD4^-CD8^-CFSE^+$ T cells compared with controls (no BM-MSC; 7.16% ± 3.14%), suggesting modulation of T-cell differentiation to alternate subsets outside of the helper and cytotoxic lineages (Figure 5D,E). On the contrary, NEG Naïve (6.38% ± 4.94%; $P < .01$) and NEG Primed (5.55% ± 4.84%; $P < .001$) groups showed no difference with the control, but were significantly lower than the POS group. The effects of all POS and NEG BM-MSC groups on cytotoxic T-cell differentiation were comparable to controls (30.35% ± 17.03%); however, a trend is observed with mild suppressive effects by the POS Naïve (21.51 ± 11.59) and POS Primed (17.82% ± 15.88%), not evident with the NEG Naïve (29.41 ± 9.24) and NEG Primed (28.37% ± 10.45%) cohorts.

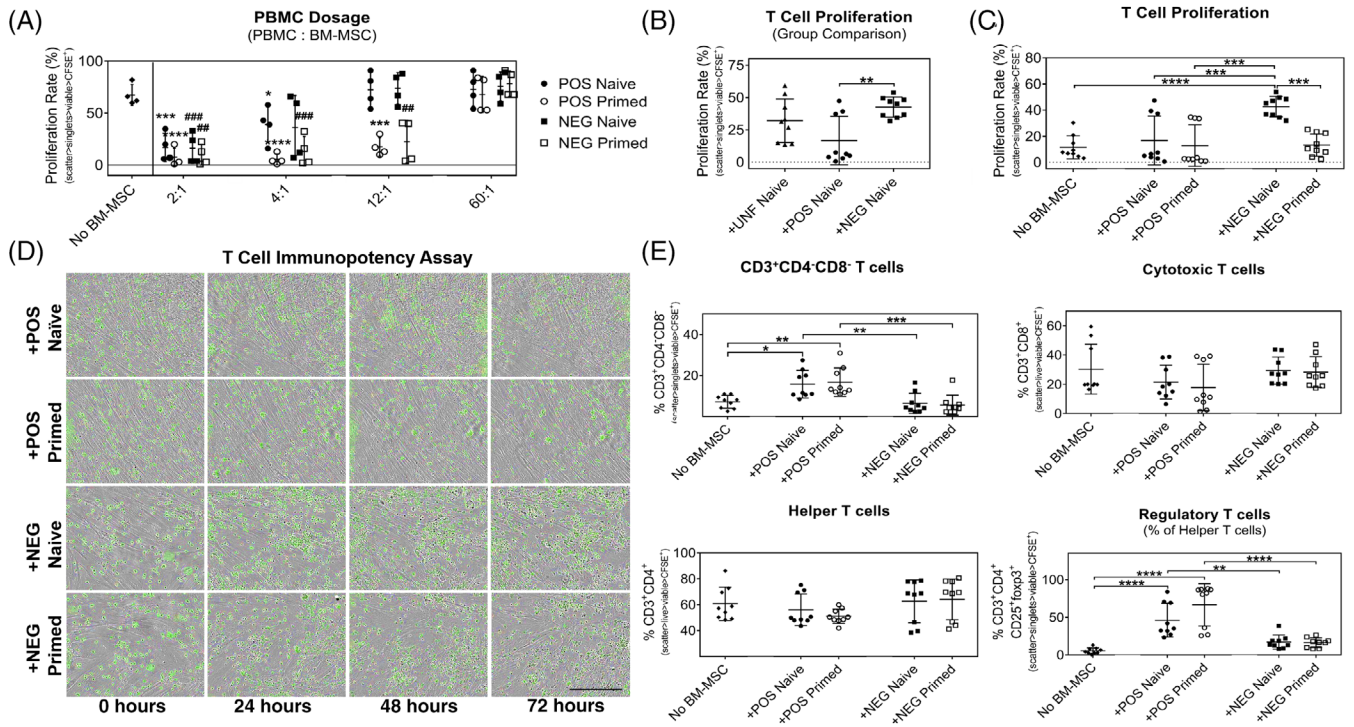

FIGURE 5 Immunopotency assays of POS and NEG cohorts reveal markedly robust potency of POS BM-MSC cohorts. A, Dosage responses of PBMCs cocultured with Naïve and Primed cohorts of POS and NEG BM-MSCs exhibit comparable effects between Naïve cohorts and Primed cohorts yet show enhanced suppressive effects between the Primed groups to the Naïve groups. B, Group comparison between UNF, POS, and NEG groups showed a significant reduction of stimulated T-cell proliferation by coculture with POS Naïve BM-MSC than NEG Naïve. C, Proliferation rates of stimulated T cells cocultured with Naïve and Primed cohorts of POS and NEG BM-MSC demonstrated the potency of the POS Naïve and POS Primed groups compared with the NEG Naïve group. D, Images of the 72-hour duration of the immunopotency assay showing the proliferation of the stimulated T cells (green) that are cocultured above the adherent BM-MSC groups. E, T-cell subsets differentially promoted by the coculture with Naïve and Primed cohorts of the POS and NEG BM-MSC. Scale bar = 500 μm. Values are presented as mean ± SD. *P < .05; **P < .01; ***P < .001; ****P < .0001. BM-MSC, bone marrow-derived mesenchymal stem/stromal cells; UNF, unfractionated

Similarly, POS Naïve (56.11% ± 12.21%) and POS Primed (51.15% ± 5.51%) BM-MSC modestly reduced differentiation of helper T cells compared with controls (60.78% ± 12.88%), while NEG Naïve (62.70% ± 16.55%) and NEG Primed (64.14% ± 15.74%) BM-MSC promoted modest differentiation of the helper T-cell subsets. More importantly, analysis of the Treg frequency within the helper T subset showed that POS Naïve (46.23% ± 22.28%; P < .0001) and POS Primed (66.66% ± 28.06%; P < .0001) induced the most significant amount compared with controls (5.56% ± 3.87%). Further, induction by POS Naïve was markedly greater (P < .01) than NEG Naïve BM-MSC (17.17% ± 9.33%), and POS Primed was significantly higher (P < .0001) than NEG Primed BM-MSC (16.30% ± 6.50%; Figure 5E). Collectively, this compelling evidence underscores the mechanistic underpinnings of immunomodulation in which the POS subpopulation outperforms the NEG subpopulation in several approaches.

2.9 | POS subpopulation ameliorates synovitis and fat pad fibrosis by promoting M2 alternative activation macrophages

In vivo therapeutic efficacy in a well-established rat model of synovium and infrapatellar fat pad (IFP) inflammation and fibrosis was evaluated by intra-articular administration of monosodium iodoacetate (MIA) inducing local inflammatory changes leading to progressive thickening of synovium (ie, synovitis) and fibrosis throughout the IFP.[54,55] As shown in the experimental outline (Figure 6A), synovitis/IFP fibrosis induction was followed 4 days later (at the peak of local inflammation[54]) by a single intra-articular injection of BM-MSC (UNF, POS, or NEG). Sham (no MIA and injection with vehicle only) and untreated (MIA induction followed by no treatment) animals were used as healthy and diseased controls, respectively. Evaluation of each group was performed by a standard semiquantitative scoring method,[54,55] where synovitis and IFP fibrosis are independently assessed (0-3 for each). The latter is then complemented by a stain-based quantitative analysis using a computational algorithm (Figure S6B).

Synovitis scores showed a significant inflammatory reaction in treated animals (n = 6) after the induction with MIA, evident when comparing Sham (0.17 ± 0.24) with the Untreated (3.00 ± 0.00; P < .0001). Treatment with UNF (1.67 ± 0.52; P < .0001), POS (1.33 ± 0.52; P < .01), and NEG (2.25 ± 0.52; P < .0001) showed significantly greater synovitis scores compared with Sham with POS treatment with the greatest amelioration. This improvement was further demonstrated by the comparison of scores against the Untreated synovitis score with the POS (P < .0001) and UNF (P < .05) treatment

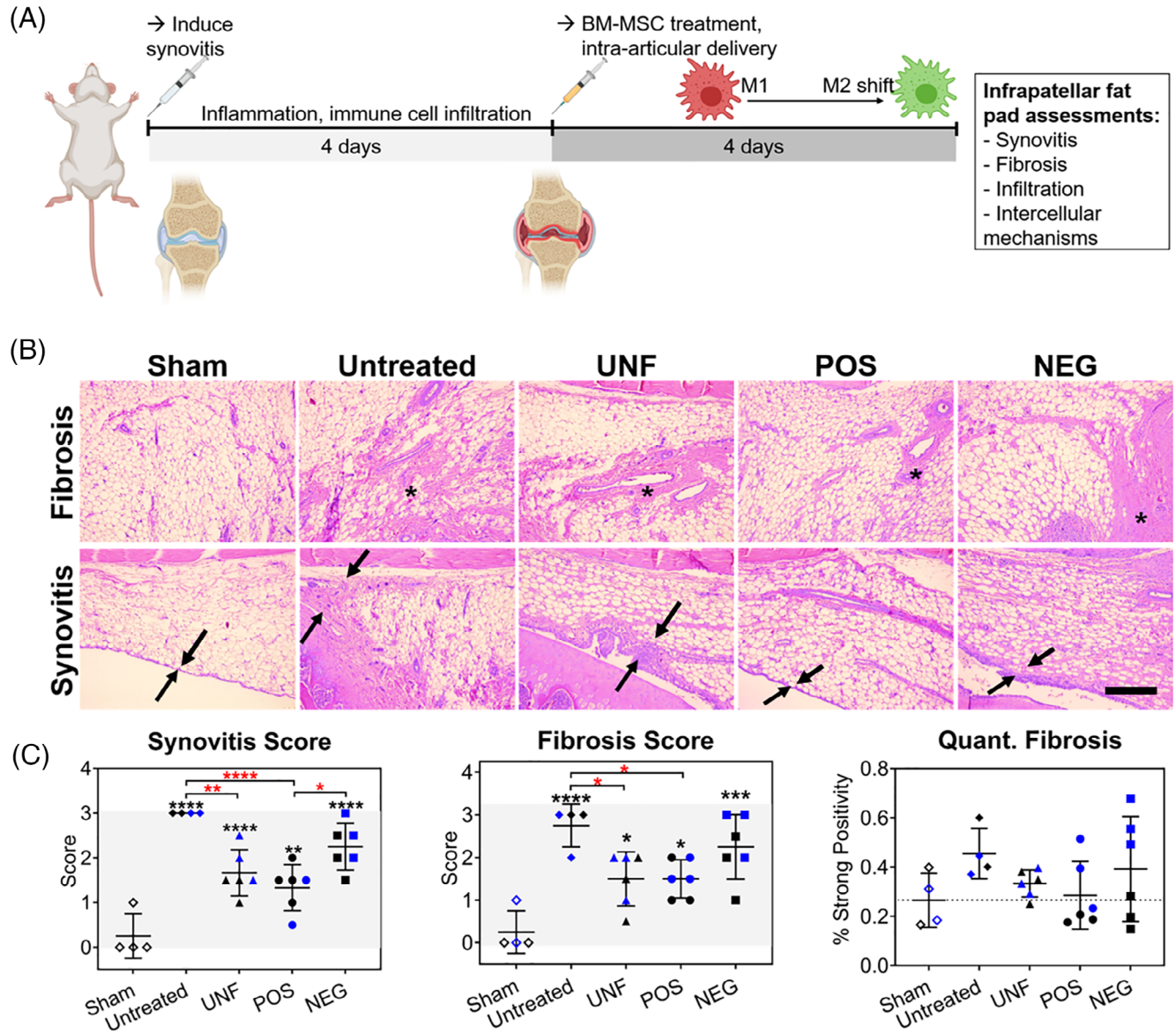

FIGURE 6 In vivo assessment of therapeutic efficacy of UNF, POS, and NEG BM-MSC following synovitis and IFP fibrosis of the knee. A, Experimental design of the in vivo induction of synovitis/IFP fibrosis, treatment with BM-MSC, and tissue assessments. Created with BioRender.com. B, H&E-stained sections of the synovium and IFP were imaged at ×4 magnification for structural changes indicative of synovitis (thickening of synovial membrane; bordered with arrows) and IFP fibrosis (dense, fibrous tissue; asterisks). Asterisks and arrows denote areas of observable fibrosis and synovitis, respectively. C, Using a standard scoring system and computational approach, quantitative comparisons of synovitis and scoring were performed. Black data points signify female animals, and blue data points signify male animals. Black asterisks denote statistical difference against Sham group, and red asterisks denote differences against untreated group. Scale bar = 200 μm. Values are presented as mean ± SD. *$P < .05$; **$P < .01$; ***$P < .001$; ****$P < .0001$. BM-MSC, bone marrow-derived mesenchymal stem/stromal cells; IFP, infrapatellar fat pad; UNF, unfractionated

markedly reduced while no difference was seen with the NEG treatment. Additionally, POS ($P < .05$) had significantly lower synovitis score than the NEG treatment group. Similar trends were apparent with the IFP fibrosis scores showing significant differences in all groups (untreated $P < .0001$; UNF $P < .05$; POS $P < .05$; NEG $P < .001$) compared with Sham (0.25 ± 0.50). Compared with the Primed group (2.75 ± 0.50), treatment with UNF (1.5 ± 0.63; $P < .05$) and POS (1.5 ± 0.45; $P < .05$) BM-MSC were markedly reduced and no differences with NEG BM-MSC (2.25 ± 0.76). Similar supporting data were obtained with the computational fibrosis quantification, which found a comparable trend as with the scoring system, with reduced fibrosis in UNF (0.33% ± 0.05%), POS (0.29% ± 0.14%) and to a lesser extent with NEG (0.39% ± 0.21%) BM-MSC compared with the Untreated (0.45% ± 0.10%). The clear trend in fibrosis evaluations, yet with no statistical differences, can be attributed to our early assessment time point (8 days after MIA induction). At this early point, unlike the established synovitis, it is expected that the fibrotic changes are variable. Furthermore, large differences were depicted

between female and male recipients that contributed to the variability (Figure 6B,C).

To determine mechanistic cellular changes promoted locally by BM-MSCs in vivo, M1/M2 macrophage phenotypic evaluations were performed (represented as the ratio of M2 over M1 for consistent comparisons), as MSCs modulate macrophage polarization.[56] Synovium/IFP resident and infiltrated macrophages have demonstrated key roles in joint health and articular cartilage degenerative changes, as they are the source of inflammatory and catabolic mediators including IFN-γ, TNF-α, IL-1,-6,-8, and metalloproteinases.[57] Classically activated-M1 ($CD86^+$) and alternatively activated-M2 ($CD206^+$) macrophages were detected within the synovium and body of the IFP, specifically surrounding the vasculature (Figure 7A,B). Differences were observed between male and female recipients, and thus the results are presented separately by gender. Furthermore, in spite of variations among recipients, consistent trends were observed. In females, M2 and M1 macrophages were comparably observed within synovium and IFP tissues of the Sham group, resulting in a 0.98 ± 0.95 M2/M1 ratio. Untreated recipients showed a reduced M2/M1 score of 0.53 ± 0.11 demonstrating the balance tipped when largely proinflammatory M1 macrophages are present. More importantly, treatment with both UNF (1.68 ± 0.98 M2/M1) and POS (1.13 ± 1.00 M2/M1) BM-MSC switched

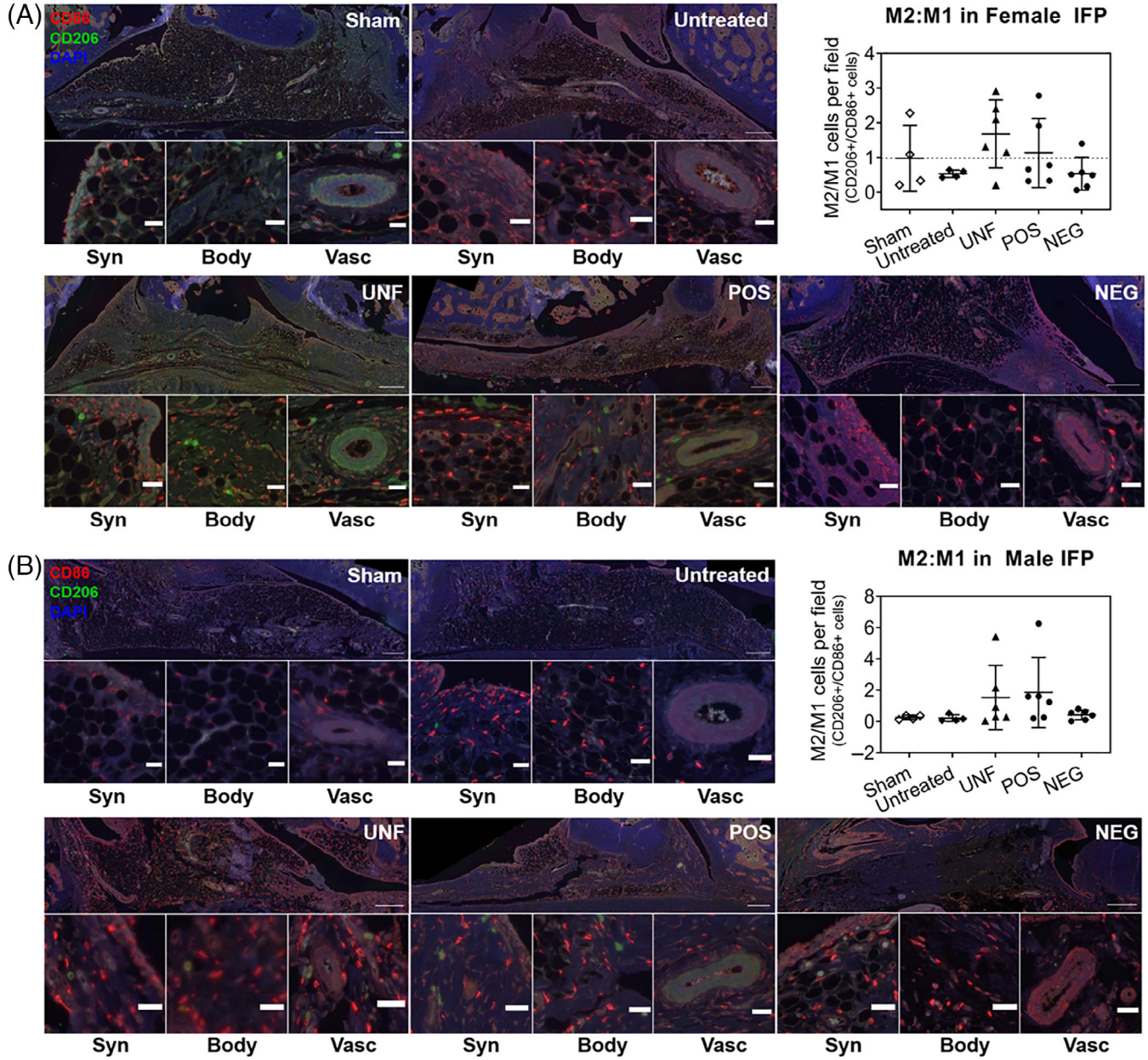

FIGURE 7 In vivo M1-to-M2 shift mediated by POS in areas of synovitis and IFP fibrosis. Images and quantification for M1 (CD86; classical activation) and M2 (CD206; alternative activation) macrophages present in, A, female and B, male knee sections in each group. M2:M1 ratios define the positive effects following treatment representing a majority of M2 over M1 macrophages. Scale bars = 500 μm (top wide-view images) and 100 μm (bottom images). IFP, infrapatellar fat pad

the ratios to positive values (ie, M2 values larger than M1 values), suggesting active macrophage polarization toward an anti-inflammatory therapeutic M2 phenotype. This remarkable improvement was not observed with NEG BM-MSC treatment (0.54 ± 0.47 M2/M1), which showed a comparable ratio to the Untreated group suggesting an inability to revert the M1 phenotype by this subpopulation (Figure 7A). Unlike females, the male Sham group (0.26 ± 0.14 M2/M2) showed little presence of M2 macrophages compared with the high presence of M1, resulting in similar values to the Untreated IFP group (0.22 ± 0.22 M2/M1). The remaining groups showed comparable results as with females, with a large induction of M2 macrophages with both UNF (1.53 ± 2.06 M2/M1) and more so POS (1.86 ± 2.24) BM-MSC treatment, and NEG BM-MSC (0.42 ± 0.31 M2/M1) undistinguishable from the Untreated group (Figure 7B).

3 | DISCUSSION

The heterogeneity and identification of distinct subpopulations within crude MSCs have been implicated to confound evidence and expected outcomes when used as biologics.[58-62] These effects may slow advancements and engender regulatory concerns even when standard methodologies are practiced. Donor-specific differences (eg, age, sex, health status) also correlate to the "cell fitness" and therapeutic efficacy adding yet another complexity among donor comparisons.[49,63,64] Previous evidence has helped distinguish subpopulations within crude MSCs based on the expression of the pericyte-related marker CD146. These include descriptions of their developmental origins,[65-68] association with the perivascular niche,[17,18,23-25,69] self-renewal and stem-like capacities supporting hematopoiesis,[26,27,29,66] and therapeutic use as osteoblastic progenitors for bone repair.[31,32] Our results further support this emerging distinction beyond those progenitor and hematopoietic support contributions for the CD146$^+$ (POS) subpopulation. Herein, we correlated phenotypic, transcriptional, and secretory signatures in response to inflammatory priming with enhanced functional potency based on immunomodulatory and anti-inflammatory effects.

Pericytes have long been associated with structural functions in blood vessels, including stabilization, tone control, angiogenesis, and permeability.[70] Additional functions such as macrophage-like properties and effects on the immune system (eg, cell trafficking and responses) have now been more clearly elucidated.[71] Our previous reports show perivascular BM-MSC function as gatekeepers during metastatic cancer cell extravasation, exercised through a CD146-mediated mechanism.[72] Suggestively, the strategic perivascular localization may foster sensing capabilities to survey, guide, and instruct cells through transendothelial trafficking. Based on these observations, we hypothesized that CD146$^+$ perivascular BM-MSC would more robustly influence immune/inflammatory cascades than their counterparts more distant from vascular structures (CD146$^-$). Such a functional discrimination has immediate repercussions not only for our understanding of MSC biology, but also to streamline manufacturing protocols for cell-based products with less heterogeneous and more predictable compositions.

To experimentally test our hypothesis, we employed an in vitro technique of inflammatory priming (TNF-α, IFN-γ exposure) to both interrogate phenotypic adaptations and examine the potency of the responses from each BM-MSC donor and associated subpopulations. The results obtained with UNF Naïve and Primed cohorts built the foundation for the subsequent evaluation of the CD146$^+$ (POS) and CD146$^-$ (NEG) subpopulations, where correlative evidence suggested the contribution of each subpopulation within the whole UNF preparation. Cell priming has been used as a strategic method to incite an analyzable response by the cells or to precondition them to augment a desired trait or effect.[73,74] Moreover, priming BM-MSC prior to performing IPAs using target cells better recapitulates the in vivo pathologic events involving active secretion of inflammatory molecules followed by cellular infiltration of immune cells (eg, T cells and PBMCs) and activation of resident cells (eg, macrophages) typical of tissue damage.[75] We found that priming UNF BM-MSC induced a consistent response among all eight donors examined regardless of age and gender. This included CD146^{high}CD107a^{high}, CD146^{high}CXCR4^{high}, and CD146^{high}LepR^{high} phenotypes, reminiscent of the perisinusoidal MSC within the BM[26,27] with highly responsive and secretory capacities. Remarkably, the sorted POS Primed subpopulation uniquely recapitulated this phenotypic enrichment, suggesting that the overall phenotypic change seen in the UNF preparation can be attributed to the POS group.

The resulting phenotype of UNF Primed BM-MSC corresponded to a transcriptional profile that indicated a more stem-like and immunomodulatory state with increased key transcripts (eg, *LIF*). Together with a highly immunomodulatory secretory profile (eg, PGE-2 and IDO activity), they were consistent with the results of the IPA that achieved robust suppression of PBMC proliferation (even at high PBMC:MSC ratios), overcoming the declining dose-dependent effect of UNF naïve cells. The deep analysis of each of the subpopulation's secretory profiles revealed that the POS was most robust in response to the inflammatory priming, strongly suggesting that the POS subpopulation, and not the NEG, are the potently responsive cells contributing to the overall effect of the UNF BM-MSC population. This aligns with the enhanced secretory potency and the higher CD107a inducible expression found in the POS group. Functionally, the POS Primed contributed more than the NEG Primed cohort to the stabilization of the PBMC proliferation suppression even at high PBMC:MSC ratios, strengthening the concept of this robustly immunosuppressive subpopulation.

The analysis of T-cell proliferation and subset differentiation showed additional compelling evidence for the immunomodulatory capacity of BM-MSCs, and specifically the POS subpopulation. The stimulus used triggers the initial activation of T cells, yet lacks perpetuating stimuli yielding only mild proliferation but induction of differentiation to the major subsets as main measurable outcomes. The expected additional proliferative response of T cells when non-stimulated UNF Naïve BM-MSCs were present[76] was explained by the effects of the NEG subpopulation exclusively, as the POS Naïve indeed suppressed T-cell proliferation effectively. Interestingly, this intrinsic immunosuppressive influence of the Naïve cohort of the POS subpopulation eliminated the need for priming, previously reported as requisite to induce immunosuppressive activities of MSC via NO/IDO

and monocyte presence.[56,76-78] It also provides information to substantiate the physiological distinction of MSC into types 1 and 2, which largely depends on the absence or presence of an IFN-γ/TNF-α-rich environment they sense, respectively.[9,56] Priming demonstrated a marked suppression of T-cell proliferation in all groups (ie, UNF Primed, POS Primed, and NEG Primed) comparable to the effect of the POS Naïve group. Beyond these distinct effects on overall T-cell proliferation, specific and significant differences were also generated by POS and NEG groups in the subset composition of T cells. The robust induction of Tregs and $CD3^+CD4^-CD8^-$ T cells exclusive of the POS group, supports the fact that MSC are known to shift the T-cell axis from cytotoxic to Tregs for reparative and tolerogenic effects.[79,80] However, now clarifying the identity of the cells responsible for that shift (POS), and their innate potency to exert that effect even without prior cues/priming. An overall attenuation of T-cell differentiation provides a fundamental mechanism of BM-MSC immunomodulatory effects necessary to translate for therapeutic use.

UNF Primed BM-MSC also showed downregulation of the multilineage differentiation master genes *RUNX2*, *SOX9*, and *PPARγ*. With priming, these findings suggestively enabled a controlled shift toward stemness and immunomodulation and away from progenitor capabilities, which coincides with the inherent characteristic of asymmetrical division of MSC. However, the skewed differentiation programs (especially osteogenic and adipogenic) were initially difficult to reconcile with the observed CD146 and LepR enriched phenotype after priming based on the previous reported osteogenic nature of $CD146^+$ perivascular osteoprogenitors[29] and PSC,[31-33] as well as $LepR^+$ adipogenic progenitors.[53] The apparent dichotomy was elucidated after analyzing the transcriptional profiles of the sorted and Primed POS and NEG subpopulations. Downregulation of *RUNX2* and *PPARγ*, along with other key transcripts responsible for healthy osteogenic and adipogenic programs were exclusively shared between UNF and NEG groups, leaving POS with no alterations in those molecular programs. Consequently, the compromised differentiation potential of the NEG subpopulation upon priming suggests the POS subpopulation is the functional subset capable of exerting a spectrum function not limited to the environment they sense.

Relevant to translational efforts, all the in vitro functional discrimination between POS and NEG was successfully translated in vivo. Intra-articular injection of POS BM-MSC therapeutically outperformed NEG cohorts, greatly improving synovitis and IFP fibrosis within the joint, correlative to promoting rapid M2-macrophage phenotypic shift. Macrophages are prominently influential cells in various milieus given their orchestrating roles regulating local reparative changes, thus becoming therapeutic cell targets. In fact, a triangulation involving MSCs, macrophages, and T cells has been described by François et al.[78] They show that MSC-derived IDO activity drives the M2 polarization of macrophages, which in turn helps suppress T-cell proliferation thus amplifying the MSC effect. Moreover, M2 macrophage polarization counteracts the secretion of inflammatory and catabolic molecules at the expense of the M1 function, reducing joint damage especially to the articular cartilage.[57,81,82] We have previously demonstrated the homing and transient engraftment (≤7 days) of MSC intra-articularly injected in this model of synovitis/IFP fibrosis.[83] Therefore, we propose that highly sensitive, secretory, and potently immunosuppressive POS BM-MSC ameliorate the inflammatory and fibrotic activities in the synovium and IFP, in part by facilitating the reparative M2 macrophage phenotypic shift.

These high-content data provided several methods of characterizing the functional potency of BM-MSCs that can be further adapted for standardization in efforts to test potency across tissue-specific MSC preparations. Sorting methods to capture greater purity between subpopulations should be implemented to overcome the limitations of MACS. Although much of the data contains significant trends, deviations among donors emphasize the need to detect donor-specific differences to better tailor potential biologics as therapies. Further investigations into the functional potency may allow for greater understanding of functional subpopulations (eg, $CD146^+$ BM-MSC) within the crude population of MSC, determining "cell fitness" representative to donor health, and ultimately predictivity of in vivo cell interactions for better alignment with expected outcomes.

4 | CONCLUSION

This study bolsters the notion of distinct MSC functional subpopulations attribute to CD146 expression, previously determined based on osteogenic potential and hematopoietic control and now includes immunomodulatory potential and therapeutic efficacy. Our data strongly supports the signature quality attributes of the $CD146^+$ subpopulation as the robust sensory/secretory/immunomodulatory cells within crude preparations. These findings have translational implications aimed to comply with rigor and transparency as well as indicate trends and tools adaptable for scale-up cell manufacturing by minimizing variability and offering a way to assess cell-based product potencies.

ACKNOWLEDGMENTS

We give great thanks to Arnold I. Caplan, PhD, and Rodrigo Somoza, PhD, for donating healthy donor BM-MSC used in our studies, and Oliver Umland, PhD, and Marcia Boulina, PhD, for their technical assistance in the Diabetes Research Institute flow cytometry and imaging core facilities. We also thank Thomas M. Best, MD, PhD, for reviewing the manuscript.

CONFLICT OF INTEREST

A.B. declared consultancy role with Xytogen Biotech, Inc. D.C. received research funding from Soffer Family Foundation; participates in the scientific advisory board of RegenMed, LLC and is a paid consultant of Lipogems USA, LLC, and Cryovida Banco de Células Madre Adultas. All of the other authors declared no potential conflicts of interest.

AUTHOR CONTRIBUTIONS

A.C.B.: conception and design, collection and assembly of the data, data analysis and interpretation, manuscript writing; D.K., M.A.W., C.P.O.: collection and assembly of the data, data analysis and interpretation; A.A.: administrative support, final approval of manuscript; D.C.: conception and design, manuscript writing, administrative support, final approval of manuscript.

DATA AVAILABILITY STATEMENT

All data contained herein was generated and represented from this original research study.

ORCID

Annie C. Bowles https://orcid.org/0000-0003-1924-8949
Carlotta Perucca Orfei https://orcid.org/0000-0001-6162-8668
Diego Correa https://orcid.org/0000-0002-9004-4300

REFERENCES

1. Caplan AI, Correa D. The MSC: an injury drugstore. *Cell Stem Cell*. 2011;9(1):11-15.
2. Salgado AJ, Gimble JM. Secretome of mesenchymal stem/stromal cells in regenerative medicine. *Biochimie*. 2013;95(12):2195.
3. Salgado AJ, Gimble JM, Costa BM. The cell secretome in personalized and regenerative medicine. *Biochimie*. 2018;155:1.
4. Caplan AI, Sorrell JM. The MSC curtain that stops the immune system. *Immunol Lett*. 2015;168(2):136-139.
5. Caplan AI. New MSC: MSCs as pericytes are sentinels and gatekeepers. *J Orthop res*. 2017;35(6):1151-1159.
6. Kehl D, Generali M, Mallone A, et al. Proteomic analysis of human mesenchymal stromal cell secretomes: a systematic comparison of the angiogenic potential. *NPJ Regener med*. 2019;4(1):8-13.
7. Salgado AJ, Sousa JC, Costa BM, et al. Mesenchymal stem cells secretome as a modulator of the neurogenic niche: basic insights and therapeutic opportunities. *Front Cell Neurosci*. 2015;9:249.
8. Kouroupis D, Sanjurjo-Rodriguez C, Jones E, Correa D. Mesenchymal stem cell functionalization for enhanced therapeutic applications. *Tissue Eng Part B Rev*. 2019;25(1):55-77.
9. Waterman RS, Tomchuck SL, Henkle SL, Betancourt AM. A new mesenchymal stem cell (MSC) paradigm: polarization into a pro-inflammatory MSC1 or an immunosuppressive MSC2 phenotype. *PLoS One*. 2010;5(4):e10088.
10. Waterman RS, Morgenweck J, Nossaman BD, Scandurro AE, Scandurro SA, Betancourt AM. Anti-inflammatory mesenchymal stem cells (MSC2) attenuate symptoms of painful diabetic peripheral neuropathy. *Stem Cells Translational Medicine*. 2012;1(7):557-565.
11. Tomchuck SL, Zwezdaryk KJ, Coffelt SB, Waterman RS, Danka ES, Scandurro AB. Toll-like receptors on human mesenchymal stem cells drive their migration and immunomodulating responses. *Stem Cells*. 2008;26(1):99-107.
12. Dominici M, Le Blanc K, Mueller I, et al. Minimal criteria for defining multipotent mesenchymal stromal cells. The International Society for Cellular Therapy position statement. *Cytotherapy*. 2006;8(4):315-317.
13. Krampera M, Galipeau J, Shi Y, Tarte K, Sensebe L, MSC Committee of the International Society for Cellular Therapy (ISCT). Immunological characterization of multipotent mesenchymal stromal cells—the International Society for Cellular Therapy (ISCT) working proposal. *Cytotherapy*. 2013;15(9):1054-1061.
14. Horwitz EM, Le Blanc K, Dominici M, et al. Clarification of the nomenclature for MSC: the International Society for Cellular Therapy position statement. *Cytotherapy*. 2005;7(5):393-395.
15. Caplan AI. Mesenchymal stem cells: time to change the name!*Stem Cells Translational Medicine*. 2017;6(6):1445-1451.
16. da Silva Meirelles L, Sand TT, Harman RJ, Lennon DP, Caplan AI. MSC frequency correlates with blood vessel density in equine adipose tissue. *Tissue Eng Part A*. 2009;15(2):221-229.
17. Corselli M, Crisan M, Murray IR, et al. Identification of perivascular mesenchymal stromal/stem cells by flow cytometry. *Cytometry A*. 2013;83(8):714-720.
18. Crisan M, Yap S, Casteilla L, et al. A perivascular origin for mesenchymal stem cells in multiple human organs. *Cell Stem Cell*. 2008;3(3):301-313.
19. da Silva Meirelles L, Caplan AI, Nardi NB. In search of the in vivo identity of mesenchymal stem cells. *Stem Cells*. 2008;26(9):2287-2299.
20. Schwab KE, Gargett CE. Co-expression of two perivascular cell markers isolates mesenchymal stem-like cells from human endometrium. *Hum Reprod*. 2007;22(11):2903-2911.
21. Gomes JP, Coatti GC, Valadares MC, et al. Human adipose-derived CD146+ stem cells increase life span of a muscular dystrophy mouse model more efficiently than mesenchymal stromal cells. *DNA Cell Biol*. 2018;37(9):798-804.
22. Chan CKF, Gulati GS, Sinha R, et al. Identification of the human skeletal stem cell. *Cell*. 2018;175(1):43-56.
23. Tormin A, Li O, Brune JC, et al. CD146 expression on primary nonhematopoietic bone marrow stem cells is correlated with in situ localization. *Blood*. 2011;117(19):5067-5077.
24. Corselli M, Chin CJ, Parekh C, et al. Perivascular support of human hematopoietic stem/progenitor cells. *Blood*. 2013;121(15):2891-2901.
25. Espagnolle N, Guilloton F, Deschaseaux F, Gadelorge M, Sensébé L, Bourin P. CD146 expression on mesenchymal stem cells is associated with their vascular smooth muscle commitment. *J Cell Mol Med*. 2014;18(1):104-114.
26. Mendelson A, Frenette PS. Hematopoietic stem cell niche maintenance during homeostasis and regeneration. *Nat Med*. 2014;20(8):833-846.
27. Méndez-Ferrer S, Michurina TV, Ferraro F, et al. Mesenchymal and haematopoietic stem cells form a unique bone marrow niche. *Nature*. 2010;466(7308):829-834.
28. Zhou BO, Yue R, Murphy MM, Peyer JG, Morrison SJ. Leptin-receptor-expressing mesenchymal stromal cells represent the main source of bone formed by adult bone marrow. *Cell Stem Cell*. 2014;15(2):154-168.
29. Sacchetti B, Funari A, Michienzi S, et al. Self-renewing osteoprogenitors in bone marrow sinusoids can organize a hematopoietic microenvironment. *Cell*. 2007;131(2):324-336.
30. Corselli M, Chen C-W, Sun B, Yap S, Rubin JP, Péault B. The tunica adventitia of human arteries and veins as a source of mesenchymal stem cells. *Stem Cells Dev*. 2012;21(8):1299-1308.
31. James AW, Hindle P, Murray IR, et al. Pericytes for the treatment of orthopedic conditions. *Pharmacol Ther*. 2017;171:93-103.
32. James AW, Zara JN, Zhang X, et al. Perivascular stem cells: a prospectively purified mesenchymal stem cell population for bone tissue engineering. *Stem Cells Translational Medicine*. 2012;1(6):510-519.
33. Wang Y, Xu J, Chang L, et al. Relative contributions of adipose-resident CD146+ pericytes and CD34+ adventitial progenitor cells in bone tissue engineering. *NPJ Regener Med*. 2019;4(1):1.
34. Vego H, Sand KL, Hoglund RA, et al. Monomethyl fumarate augments NK cell lysis of tumor cells through degranulation and the upregulation of NKp46 and CD107a. *Cell Mol Immunol*. 2016;13(1):57-64.
35. Kannan K, Stewart RM, Bounds W, et al. Lysosome-associated membrane proteins h-LAMP1 (CD107a) and h-LAMP2 (CD107b) are activation-dependent cell surface glycoproteins in human peripheral blood mononuclear cells which mediate cell adhesion to vascular endothelium. *Cell Immunol*. 1996;171(1):10-19.
36. York VA, Milush JM. Ex vivo human natural killer (NK) cell stimulation and intracellular IFNγ and CD107a cytokine staining. *Bio-Protocology*. 2015;5(12):e1501.
37. Sudworth A, Dai KZ, Vaage JT, Kveberg L. Degranulation response in cytotoxic rat lymphocytes measured with a novel CD107a antibody. *Front Immunol*. 2016;7(9):572.
38. Wattrang E, Dalgaard TS, Norup LR, Kjærup RB, Lunden A, Juul-Madsen HR. CD107a as a marker of activation in chicken cytotoxic T cells. *J Immunol Methods*. 2015;419:35-47.
39. Alter G, Malenfant JM, Altfeld M. CD107a as a functional marker for the identification of natural killer cell activity. *J Immunol Methods*. 2004;294(1–2):15-22.

40. Liu X, Duan B, Cheng Z, et al. SDF-1/CXCR4 axis modulates bone marrow mesenchymal stem cell apoptosis, migration and cytokine secretion. *Protein Cell*. 2011;2(10):845-854.
41. Friedman JM, Halaas JL. Leptin and the regulation of body weight in mammals. *Nature*. 1998;395(6704):763-770.
42. Ducy P, Amling M, Takeda S, et al. Leptin inhibits bone formation through a hypothalamic relay: a central control of bone mass. *Cell*. 2000;100(2):197-207.
43. Scheller EL, Song J, Dishowitz MI, Soki FN, Hankenson KD, Krebsbach PH. Leptin functions peripherally to regulate differentiation of mesenchymal progenitor cells. *STEM CELLS*. 2010;28(6):1071-1080.
44. Metcalfe SM, Strom TB, Williams A, Fahmy TM. Multiple sclerosis and the LIF/IL-6 Axis: use of nanotechnology to harness the tolerogenic and reparative properties of LIF. *Nanobiomedicine*. 2015;2:5.
45. Nasef A, Mazurier C, Bouchet S, et al. Leukemia inhibitory factor: role in human mesenchymal stem cells mediated immunosuppression. *Cell Immunol*. 2008;253(1–2):16-22.
46. Jiao J, Milwid JM, Yarmush ML, Parekkadan B. A mesenchymal stem cell potency assay. *Methods Mol Biol*. 2011;677:221-231.
47. Solchaga LA, Zale EA. Prostaglandin E2: a putative potency indicator of the immunosuppressive activity of human mesenchymal stem cells. *Am J Stem Cells*. 2012;1(2):138-145.
48. Chinnadurai R, Rajan D, Qayed M, et al. Potency analysis of mesenchymal stromal cells using a combinatorial assay matrix approach. *Cell Rep*. 2018;22(9):2504-2517.
49. Scruggs BA, Semon JA, Zhang X, et al. Age of the donor reduces the ability of human adipose-derived stem cells to alleviate symptoms in the experimental autoimmune encephalomyelitis mouse model. *STEM CELLS TRANSLATIONAL MEDICINE*. 2013;2(10):797-807.
50. Trickett A, Kwan YL. T cell stimulation and expansion using anti-CD3/CD28 beads. *J Immunol Methods*. 2003;275(1–2):251-255.
51. Zhou Y, Day A, Haykal S, Keating A, Waddell TK. Mesenchymal stromal cells augment CD4+ and CD8+ T-cell proliferation through a CCL2 pathway. *Cytotherapy*. 2013;15(10):1195-1207.
52. Parish CR. Fluorescent dyes for lymphocyte migration and proliferation studies. *Immunol Cell Biol*. 1999;77(6):499-508.
53. Yue R, Zhou BO, Shimada IS, Zhao Z, Morrison SJ. Leptin receptor promotes adipogenesis and reduces osteogenesis by regulating mesenchymal stromal cells in adult bone marrow. *Cell Stem Cell*. 2016;18(6):782-796.
54. Takahashi I, Matsuzaki T, Kuroki H, Hoso M. Induction of osteoarthritis by injecting monosodium iodoacetate into the patellofemoral joint of an experimental rat model. *PLoS One*. 2018;13(4):e0196625.
55. Udo M, Muneta T, Tsuji K, et al. Monoiodoacetic acid induces arthritis and synovitis in rats in a dose- and time-dependent manner: proposed model-specific scoring systems. *Osteoarthr Cartil*. 2016;24(7):1284-1291.
56. Bernardo ME, Fibbe WE. Mesenchymal stromal cells: sensors and switchers of inflammation. *Cell Stem Cell*. 2013;13(4):392-402.
57. Bondeson J, Blom AB, Wainwright S, Hughes C, Caterson B, van den Berg WB. The role of synovial macrophages and macrophage-produced mediators in driving inflammatory and destructive responses in osteoarthritis. *Arthritis Rheum*. 2010;62(3):647-657.
58. Phinney DG. Functional heterogeneity of mesenchymal stem cells: implications for cell therapy. *J Cell Biochem*. 2012;113(9):2806-2812.
59. Sivasubramaniyan K, Harichandan A, Boss P, Buehring HJ, van Osch G. Isolation of phenotypically and functionally distinct endogeneous human bone marrow-derived mesenchymal stem/stromal cell subsets. *Osteoarthr Cartil*. 2016;24:S464.
60. Sivasubramaniyan K, Lehnen D, Ghazanfari R, et al. Phenotypic and functional heterogeneity of human bone marrow- and amnion-derived MSC subsets. *Ann N Y Acad Sci*. 2012;1266(1):94-106.
61. Buhring H-J, Treml S, Cerabona F, De Zwart P, Kanz L, Sobiesiak M. Phenotypic characterization of distinct human bone marrow-derived MSC subsets. *Ann N Y Acad Sci*. 2009;1176(1):124-134.
62. Siegel G, Kluba T, Hermanutz-Klein U, Bieback K, Northoff H, Schäfer R. Phenotype, donor age and gender affect function of human bone marrow-derived mesenchymal stromal cells. *BMC Med*. 2013;11(1):146.
63. Yu JM, Wu X, Gimble JM, Guan X, Freitas MA, Bunnell BA. Age-related changes in mesenchymal stem cells derived from rhesus macaque bone marrow. *Aging Cell*. 2011;10(1):66-79.
64. Frazier T, Lee S, Bowles A, et al. Gender and age-related cell compositional differences in C57BL/6 murine adipose tissue stromal vascular fraction. *Adipocyte*. 2018;7(3):183-189.
65. Slukvin II, Kumar A. The mesenchymoangioblast, mesodermal precursor for mesenchymal and endothelial cells. *Cell Mol Life Sci*. 2018;75:3507-3520.
66. Sacchetti B, Funari A, Remoli C, et al. No identical "mesenchymal stem cells" at different times and sites: human committed progenitors of distinct origin and differentiation potential are incorporated as adventitial cells in microvessels. *Stem Cell Rep*. 2016;6(6):897-913.
67. Maijenburg MW, Kleijer M, Vermeul K, et al. The composition of the mesenchymal stromal cell compartment in human bone marrow changes during development and aging. *Haematologica*. 2012;97(2):179-183.
68. Corselli M, Chen C-W, Crisan M, Lazzari L, Péault B. Perivascular ancestors of adult multipotent stem cells. *Arterioscler Thromb Vasc Biol*. 2010;30(6):1104-1109.
69. Covas DT, Panepucci RA, Fontes AM, et al. Multipotent mesenchymal stromal cells obtained from diverse human tissues share functional properties and gene-expression profile with CD146+ perivascular cells and fibroblasts. *Exp Hematol*. 2008;36(5):642-654.
70. Díaz-Flores L, Gutiérrez R, Madrid JF, Varela H, et al. Pericytes. Morphofunction, interactions and pathology in a quiescent and activated mesenchymal cell niche. *Histol Histopathol*. 2009;24(7):909-969.
71. Navarro R, Compte M, Álvarez-Vallina L, Sanz L. Immune regulation by pericytes: modulating innate and adaptive immunity. *Front Immunol*. 2016;7:480.
72. Correa D, Somoza RA, Lin P, Schiemann WP, Caplan AI. Mesenchymal stem cells regulate melanoma cancer cells extravasation to bone and liver at their perivascular niche. *Int J Cancer*. 2016;138(2):417-427.
73. Silva LHA, Antunes MA, Santos Dos CC, et al. Strategies to improve the therapeutic effects of mesenchymal stromal cells in respiratory diseases. *Stem Cell Res Ther*. 2018;9(1):45.
74. Kadle RL, Abdou SA, Villarreal-Ponce AP, et al. Microenvironmental cues enhance mesenchymal stem cell-mediated immunomodulation and regulatory T-cell expansion. *PLoS One*. 2018;13(3):e0193178.
75. Julier Z, Park AJ, Briquez PS, Martino MM. Promoting tissue regeneration by modulating the immune system. *Acta Biomater*. 2017;53:13-28.
76. Li W, Ren G, Huang Y, et al. Mesenchymal stem cells: a double-edged sword in regulating immune responses. *Cell Death Differ*. 2012;19(9):1505-1513.
77. Stagg J, Galipeau J. Mechanisms of immune modulation by mesenchymal stromal cells and clinical translation. *Curr Mol Med*. 2013;13(5):856-867.
78. François M, Romieu-Mourez R, Li M, Galipeau J. Human MSC suppression correlates with cytokine induction of indoleamine 2,3-dioxygenase and bystander M2 macrophage differentiation. *Mol Ther*. 2012;20(1):187-195.
79. Li J, Tan J, Martino MM, Lui KO. Regulatory T-cells: potential regulator of tissue repair and regeneration. *Front Immunol*. 2018;9:585.
80. Miyagawa I, Nakayamada S, Nakano K, et al. Induction of regulatory T cells and its regulation with insulin-like growth factor/insulin-like

growth factor binding protein-4 by human mesenchymal stem cells. *J Immunol*. 2017;199(5):1616-1625.
81. Eymard F, Pigenet A, Citadelle D, et al. Induction of an inflammatory and prodegradative phenotype in autologous fibroblast-like synoviocytes by the infrapatellar fat pad from patients with knee osteoarthritis. *Arthritis Rheumatol*. 2014;66(8):2165-2174.
82. Bartok B, Firestein GS. Fibroblast-like synoviocytes: key effector cells in rheumatoid arthritis. *Immunol Rev*. 2010;233(1):233-255.
83. Kouroupis D, Bowles AC, Willman MA, et al. Infrapatellar fat pad-derived MSC response to inflammation and fibrosis induces an immunomodulatory phenotype involving CD10-mediated substance P degradation. *Sci Rep*. 2019;9(1):1-16.

SUPPORTING INFORMATION

Additional supporting information may be found online in the Supporting Information section at the end of this article.

How to cite this article: Bowles AC, Kouroupis D, Willman MA, Perucca Orfei C, Agarwal A, Correa D. Signature quality attributes of CD146$^+$ mesenchymal stem/stromal cells correlate with high therapeutic and secretory potency. *Stem Cells*. 2020;38:1034–1049. https://doi.org/10.1002/stem.3196